Available online at www.sciencedirect.com
ScienceDirect
Journal of Power Sources 160 (2006) 1242–1250
JOURNAL OF POWER SOURCES
www.elsevier.com/locate/jpowsour

Effect of sub-freezing temperatures on a PEM fuel cell performance, startup and fuel cell components

Qiangu Yan [a,*], Hossein Toghiani [b], Young-Whan Lee [a], Kaiwen Liang [b], Heath Causey [a]

[a] *Center for Advanced Vehicular Systems (CAVS), Box 5405, Mississippi State University, MS 39762-5405, United States*
[b] *Dave C. Swalm School of Chemical Engineering, Box 9595, Mississippi State University, MS 39762, United States*

Received 23 December 2005; received in revised form 14 February 2006; accepted 14 February 2006
Available online 29 March 2006

Abstract

The cold-start behavior and the effect of sub-zero temperatures on fuel cell performance were studied using a 25-cm^2 proton exchange membrane fuel cell (PEMFC). The fuel cell system was housed in an environmental chamber that allowed the system to be subjected to temperatures ranging from sub-freezing to those encountered during normal operation. Fuel cell cold-start was investigated under a wide range of operating conditions. The cold-start measurements showed that the cell was capable of starting operation at −5 °C without irreversible performance loss when the cell was initially dry. The fuel cell was also able to operate at low environmental temperatures, down to −15 °C. However, irreversible performance losses were found if the cell cathode temperature fell below −5 °C during operation. Freezing of the water generated by fuel cell operation damaged fuel cell internal components. Several low temperature failure cases were investigated in PEM fuel cells that underwent sub-zero start and operation from −20 °C. Cell components were removed from the fuel cells and analyzed with scanning electron microscopy (SEM). Significant damage to the membrane electrode assembly (MEA) and backing layer was observed in these components after operation below −5 °C. Catalyst layer delamination from both the membrane and the gas diffusion layer (GDL) was observed, as were cracks in the membrane, leading to hydrogen crossover. The membrane surface became rough and cracked and pinhole formation was observed in the membrane after operation at sub-zero temperatures. Some minor damage was observed to the backing layer coating Teflon and binder structure due to ice formation during operation.

Keywords: Sub-freezing; PEM fuel cell; Start-up; MEA; Degradation; SEM

1. Introduction

Proton exchange membrane fuel cells (PEMFCs) have attracted great attention in recent years as a promising replacement for traditional engines due to their high power density and ultra-low emission features [1–3]. Fuel cells also offer an opportunity to use an almost limitless fuel: hydrogen. Performance with increased stability and reliability as well as low cost must be realized before fuel cells can replace internal combustion engines [4]. PEM fuel cells usually operate at temperatures between 70 and 80 °C. However, in automotive applications, PEM fuel cells will be exposed to a wider range of temperature, including sub-zero temperatures. Therefore, PEMFCs must be able to operate under these conditions that might be found in colder climates. One potential problem is that water present in the fuel cell could freeze when the fuel cell temperature drops below 0 °C. Since power generation efficiency is low at temperatures below the normal operating temperature, starting the fuel cell from low temperature is quite difficult. Moreover, prolonged exposure of the fuel cell to sub-freezing temperatures may result in ice formation. This could potentially damage the internal structure and components of the fuel cell. During fuel cell cold start and sub-freezing operation, the water generated initially at the cathode will freeze. This can block the pathways through the porous gas diffusion layer and catalyst layer, thereby, preventing the movement of reactants. Sub-zero freezing operation of fuel cell systems is an important concern; however, limited research efforts have focused on this area. The effect of water freezing on the PEMFC performance and its effect on PEMFC components have been examined by theoretical models [5–8], experimental methods [9–16], and fuel cell design optimization efforts [17–19]. Seshadri and Kabir [5] developed both steady

* Corresponding author. Tel.: +1 662 325 5906; fax: +1 662 325 5433.
E-mail address: yan@cavs.msstate.edu (Q. Yan).

0378-7753/$ – see front matter © 2006 Elsevier B.V. All rights reserved.
doi:10.1016/j.jpowsour.2006.02.075

state and transient models of a PEM fuel cell power plant for transportation applications. The results of the power plant performance testing indicated good agreement with these models. Testing showed that the power plant achieved stable performance at all power levels, including low power holds. Gummalla et al. [6] reported a study of bootstrap start using physics-based dynamic models. These models included a detailed fuel cell model, a semi-detailed stack model, and a system-level stack model. The detailed model captured the strongly coupled reaction and transport through the various sub-layers in a PEM fuel cell, namely the gas diffusion layers, catalyst layers and the polymer membrane. Comparison of model predictions and experimental data for voltage response during bootstrap start showed reasonable agreement, validating the modeling approach. The model was then deployed to analyze the startup behavior from sub-freezing conditions. The model predictions of startup temperature dynamics and the voltage response were in good agreement with the test data. These models were used for conceptual and detailed design of fuel cell stacks and power plant system. The research of Sundaresan and Moore [7] focused on the development and use of a sub-freezing thermal model for a polymer electrolyte fuel cell stack. Specifically, the work focused on the generation of a model in which the fuel cell was separated into layers to determine an accurate temperature distribution within the stack. The layered model revealed the effect of the endplate thermal mass on the end cells, and accommodated the evaluation of internal heating methods that may mitigate this effect. To investigate the basic cold-start behavior under isothermal conditions, Oszcipok et al. [8] used statistical analysis to study operational influences on the cold-start behavior of PEM fuel cells. Their regression showed that the initial current mainly depended on the membrane humidity and the operating voltage. Cho et al. [9,10] investigated the effects of freezing/thermal cycles from 80 to −10 °C on PEMFC performance. They found that the cell performance was degraded due to the phase transformation and volume changes of water during thermal cycling. The effect of water removal on PEMFC performance degradation was also examined under freezing/thermal cycles [10]. The performance degradation rate was reduced to 0.06 or −0.47%, if water was removed from the PEMFC with dry gas or with an antifreeze solution, respectively. Cargnelli et al. [11] operated a 50 W PEMFC system in a climatic chamber at −42 °C. For startup, they used a catalytic burner to heat up and humidify the reaction air. Chu et al. [12] operated a 50 W fuel cell system at −10 °C for 9 h. Datta and Velayutham reported results of a 500 W fuel cell system which was operated without any problems in the Antarctic [13]. Kagami et al. [14–16] performed non-isothermal, galvanostatic single fuel cell experiments below 0 °C. At constant gas flow, they reported that the cathode electrode surface area was reduced by ice formation, and as a result, the reaction was inhibited. With the empirical assumption that the cathode surface area was diminished in proportion to the amount of frozen water, simulations were performed which described the voltage decay over time and correlated well with experimental results. Beneficial for cold starts are low current densities which prevent voltage decay by freezing of product water. There are over 200 patents concerning fuel cell startup and operation at sub-zero temperatures. Some of these focus on improving fuel cell sub-zero start up and operation by fuel cell design optimization [17–19]. Though significant progress was achieved during recent years, more work is required in these areas including modeling, experimental measurements and fuel cell design optimization based on a judicious selection of available approaches [20].

In this work, experimental studies were directed towards identifying the impact of operating variables through changes in fuel cell performance and by examination of fuel cell components after loss of performance had been established. In these initial experiments, a 25 cm^2 fuel cell was employed. The fuel cell system was housed in an environmental chamber that allowed the system to be subjected to temperatures ranging from sub-freezing conditions to those encountered during normal operation. Care was taken to ensure that the entering feed gas streams had sufficient residence time to thermally equilibrate at the temperature of the environmental chamber. During operation at sub-freezing temperatures, humidification was not employed. Cell voltage measurements under load as a function of time from different sub-freezing starting conditions provided information regarding the minimum current density that could be realized without significant degradation in cell voltage. Changes in surface morphology, and MEA structure were analyzed by microscope analysis.

2. Experimental

2.1. Preparation of MEA and assembly of single cell

The catalyst ink for the electrodes was prepared by mixing the catalyst powder (20 wt% Pt/C, E-Tek), Nafion solution, and isopropyl alcohol. The prepared catalyst ink was then sprayed on the wet-proofed carbon paper and carbon cloth with a platinum loading of 0.4 mg cm^{-2} for both anode and cathode. The membrane electrode assembly (MEA) was fabricated by placing the electrodes on both sides of the pretreated Nafion 112, 115 and 117 membranes, followed by hot pressing at 140 °C and 200 kg cm^{-2} for 4 min. The active electrode area was 25 cm^2. A 25 cm^2 single cell was constructed from the prepared MEA, Teflon gasket and flow-field plates on both sides of the MEA and then placed in the environmental chamber to control the cell temperature from 80 to −15 °C.

2.2. Performance of fuel cell under sub-zero temperature

The effect of sub-zero temperatures on the cell performance was studied by measuring the polarization curve of the cell. The single cell was first operated at room temperature. After stabilization of cell performance was achieved at room temperature, the temperature of the chamber was lowered to the desired temperature while the fuel cell was operating. The operating system was allowed to stabilize at the desired temperature for at least 1 h prior to measurement of the polarization curve. The polarization curves of the fuel cell and the cathode temperature were recorded during operation. The polarization curve of the cell was measured at ambient temperature between each of the measurements at lower temperature. A comparison of the polarization

curve taken at ambient conditions immediately before operation at the sub-zero temperature to the polarization curve taken at ambient conditions immediately after operation at the sub-zero temperature was performed in order to reveal any possible irreversible performance losses due to water freezing inside the cell. The polarization curves were measured by scanning the current from 0 to 750 mA cm^{-2} with 20 mA increments and simultaneously measuring the cell voltage. The voltage was allowed to stabilize for 30 s at each measurement point before the next current increment. Before each polarization curve measurement, the cell was allowed to stabilize at the average current density of 100 mA cm^{-2} for 5 min. If the comparison of polarization curves showed a change in cell performance, the MEA and GDLs were replaced. Hydrogen and air were fed to the system, bypassing the external bubbler humidifiers. A stoichiometry of 1.2 was used for the fuel while air stoichiometry ranging from 2 to 6 was examined. The operating pressure was 1 atm.

2.3. Sub-zero start up

Cold-start measurements were performed at temperatures of −5, −10 and −15 °C. The 25 cm^2 single cell was first operated at room temperature (25 °C) or at 80 °C; and the operation continued until the cell performance stabilized. Once cell performance was stabilized, the feed gases to the anode and cathode were switched to dry nitrogen or hydrogen gas at the anode and dry air at the cathode at a gas flow rate of 300 mL min^{-1} until the cell voltage was decreased to zero. Then the environmental chamber was cooled to the desired sub-zero temperature, and kept at that temperature for 1 h, with the dry gas feed to the cathode and anode continuing. The hydrogen/air were then switched on and the cell was operated at the current density increasing from 0 to 100 or 200 mA cm^{-2}.

A number of tests were conducted to evaluate the effects of operating conditions on fuel cell startup. The 25 cm^2 single cell was first operated at room temperature. Once cell performance was stabilized, a number of different pretreatment methods were employed as the fuel cell system temperature was lowered to the desired sub-zero temperature. In a few runs, the fuel cells were purged with dry reactants, i.e., hydrogen and air to anode and cathode, respectively. In other runs, the fuel cells were purged with dry nitrogen and air. In still other runs, no purging was performed. The fuel cells were then cooled to sub-freezing temperatures that varied from about 0 °C to about −15 °C, and allowed to stabilize for 1 h. To restart the cells after the temperature had stabilized, the reactants (i.e. air and H_2) were supplied at room temperature without humidification. The effects of chamber temperature, insulation, gas purging, air stoichiometry and feed gas temperature on fuel cell startup were investigated. Performance (cell voltage), cell temperature, and success or failure, were recorded. In these tests, the current was drawn from the cell (i.e. the load) at 100 or 200 mA cm^{-2}.

2.4. Characterization of MEA

After exposure to sub-zero temperature cycling resulted in a permanent performance loss of greater than 10%, the MEA was removed from the cell. The polymer electrolyte and the electrodes were separated to allow independent examination. These components were compared with new components (labeled fresh) and with components obtained from normal operation of the fuel cell (membrane, GDL, catalyst). An assortment of characterization tools, such as SEM/EDX and TEM, were used to characterize the MEAs. In particular, characterization was focused on identifying chemical and/or physical changes that have occurred because of the sub-zero operating temperature.

3. Results

3.1. Effect of sub-zero temperatures on PEM fuel cell performance

The effect of sub-zero temperatures on the cell performance was studied by measuring the polarization curve of the cell operating at different temperatures in the environmental chamber. The polarization curves for different operating temperatures are shown in Fig. 1. Fig. 1 shows fuel cell voltage as a function of operating temperature between −15 and 80 °C with the hydrogen stoichiometric ratio of 1.2 and air stoichiometric ratio of 4. These results were obtained with no humidification of either feed gas. The polarization curves show that fuel cell performance was improved with increasing temperature from −15 to 25 °C. The best performance was realized at room temperature (25 °C). However, the cell performance decreased as the temperature increased further to 80 °C. This observation is believed to result from the balance of increasing gas diffusivity and decreasing membrane conductivity at higher temperature. It is easier to condense water vapor at a lower temperature; water flooding may hinder the gas transport in the catalyst layer and gas diffusion layer (GDL). Gas diffusivity of the fuel cell is improved with increasing cell temperature, however, membrane conductivity will decrease at high temperature since the gas relative humidity and the membrane water content decrease. As a result, the cell performance was worse when the temperature rose to 80 °C.

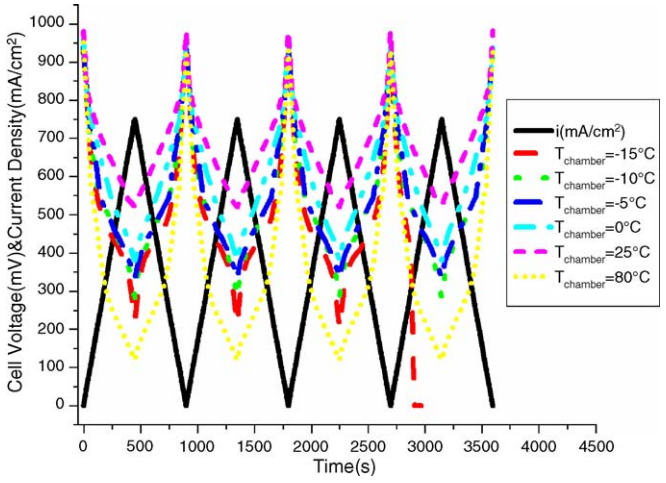

Fig. 1. Polarization curves for the 25 cm^2 fuel cell as a function of temperature.

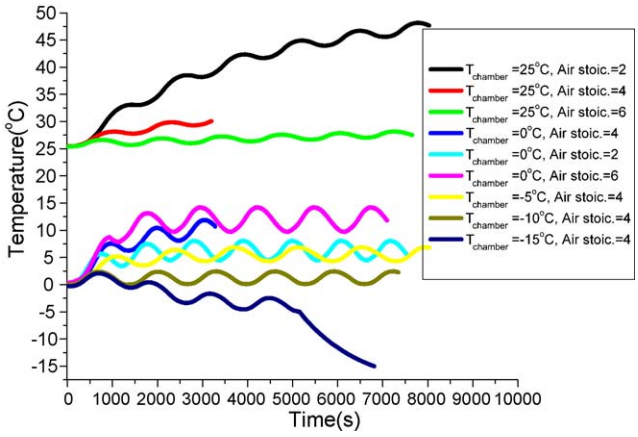

Fig. 2. Temporal variations in cell cathode temperature during operation at different environmental temperatures.

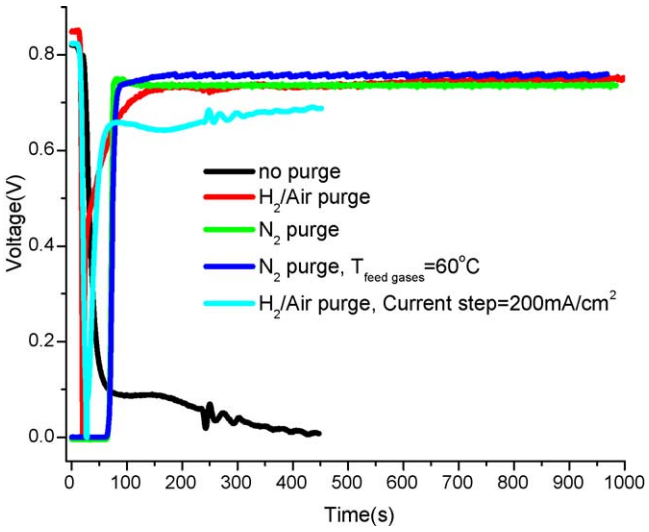

Fig. 3. Temporal variations in fuel cell voltage after startup at −5 °C.

Fuel cell performance at the chamber temperatures of 80, 25, 0, −5 and −10 °C was stable and repeatable; the polarization curves were almost identical for different cycles. However, when the chamber temperature was lowered to −15 °C, fuel cell performance was unstable. At this temperature, cell voltage decreased with increasing current–voltage (CV) cycling. After the fourth CV cycle, the cell voltage was decreased and suddenly reduced to zero at a current density of 350 mA cm^{-2}. At this point, the temperature of the cell cathode was below −5 °C.

Cell temperatures were measured on the cathode side while the polarization curves were measured and are shown in Fig. 2. Each polarization curve was obtained by scanning the current from 0 to 750 mA cm^{-2} with 20 mA increments. The temperature showed fluctuations as the current was scanned during measurement of the polarization curve. The oxygen reduction reaction (ORR) in the cathode catalyst layer will generate some amount of heat, the amount increasing with increasing current and decreasing with decreasing current; therefore, fluctuation in the cathode cell temperature when scanning the current is expected. The cell temperature increased simultaneously with the current scanning and reached a stable value about which fluctuations of between 2 and 3 °C were observed. Fuel cell cathode temperature at chamber temperatures of 25, 0, −5 and −10 °C was stable and reproducible. However, at a chamber temperature of −15 °C, the fuel cell cathode temperature was not stable; after 4 cycles, the cell cathode temperature dropped to below −5 °C, cell performance was lost irreversibly and the cathode temperature decreased sharply to the chamber temperature of −15 °C.

3.2. Cold-start measurements

Cold-start measurements were performed at chamber temperatures of −5, −10 and −15 °C. The procedure outlined in Section 2.3 sub-zero startup was followed. The fuel cell was cooled to sub-freezing temperatures that varied from about 0 °C to about −15 °C, and allowed to stabilize for 1 h. To restart the cell after freezing, the reactants (i.e. air and H_2) were supplied at room temperature without humidification.

The effects of chamber temperature, insulation, gas purging, air stoichiometry, and feed gas temperature on fuel cell startup were investigated. Performance (cell voltage), cell temperature and success or failure, were recorded. In these tests, the current was drawn from the cell (i.e. the load) at 100 or 200 mA cm^{-2}. The results of these tests are shown in Table 1.

The cold-start behavior of the cell at −5 °C is illustrated in Fig. 3, while cold-start behavior at −10 and −15 °C results are shown in Fig. 4. The cell was capable of starting operation at −5 °C without any difficulty, if the cell was pre-purged and insu-

Table 1
Cold startup cases

$T_{chamber}$ (°C)	N_2 purge	Insulate	Feed gas preheated	Air stoichiometry	Result
−5	No	No	No (RT)	2	Failure
−5	Yes	No	No (RT)	2	Failure
−5	Yes	Yes	No (RT)	2	Success
−10	Yes	Yes	No (RT)	2	Failure
−10	Yes	Yes	No (RT)	4	Success
−15	Yes	Yes	No (RT)	4	Failure
−5	Yes	No	Yes (60 °C)	2	Success
−10	Yes	No	Yes (60 °C)	2	Failure
−10	Yes	No	Yes (80 °C)	2	Success

A 25 cm^2 fuel cell, H_2 stoichiometry = 1.2, all the feed gases were dry, current density stepped from 0 to 100 mA cm^{-2} when start up.

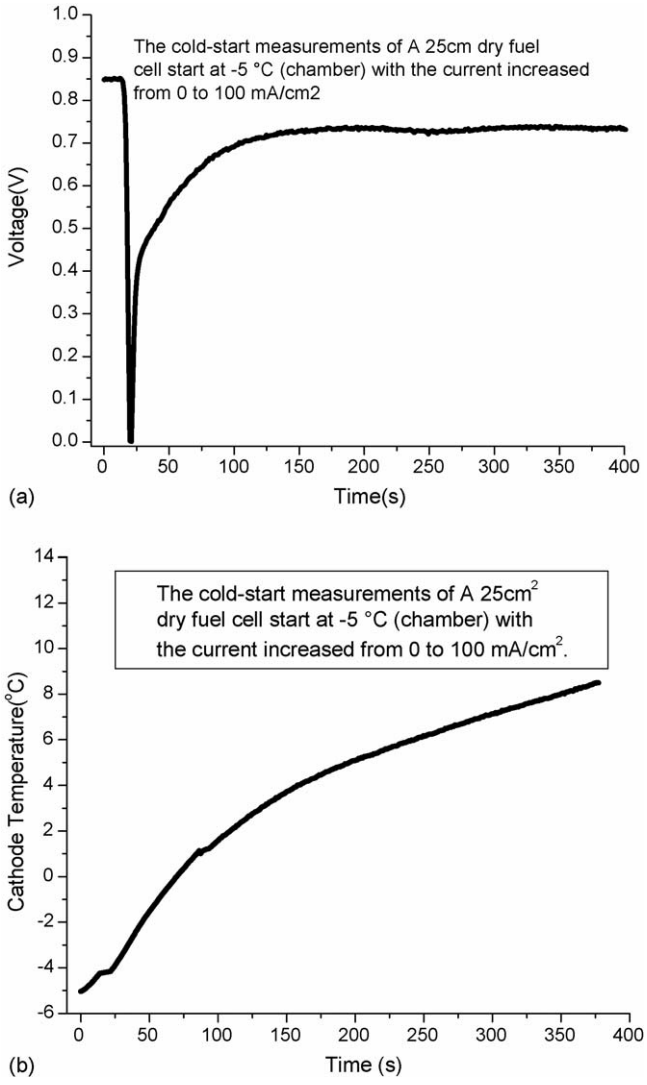

Fig. 4. Temporal variations in fuel cell voltage (a) and cell cathode temperature (b) after startup at −5 °C.

lated. If the fuel cell had been shut down without performing the purge, free water could be present on the catalyst and in the gas diffusion layers of the cell. This free water may freeze to ice when the fuel cell is subjected to sub-zero temperatures and hinder the penetration of reactants into the catalyst from the gas diffusion layer and prevent the desired chemical reaction from occurring. In this case, the fuel cell could not startup and "failure' is listed as the result in Table 1 and Fig. 3. If the cell was purged using dry H_2 and air before shutdown, and cell temperature then decreased to −5 °C, the cell was able to startup (a load was connected with current density of 100 or 200 mA cm^{-2}). During the first 20 s, the voltage sharply decreased but recovered gradually as the fuel cell temperature increased gradually (Fig. 4). Once the fuel cell had started up, the exothermic reaction of hydrogen and oxygen within the fuel cell and the resistive heating due to internal ohmic losses caused the cell temperature to rise. Preheating of feed gases to the cell also yielded successful startup of the fuel cell from sub-zero temperature (Table 1; Figs. 4 and 6 results). The preheated air carries away the water

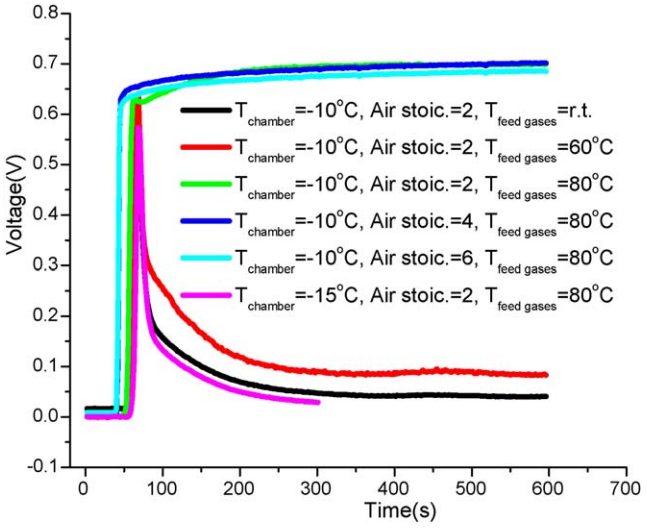

Fig. 5. Temporal variations in fuel cell voltage after startup at −10 and −15 °C.

formed in the cathode catalyst layer before it accumulates and freezes in the cell; therefore, preheating the air or increasing air flow rate will result in improved fuel cell operation at sub-zero temperatures.

The cell was capable of starting operation with the proper starting procedure at −10 °C (Fig. 5). With the higher air stoichiometry and higher feed gas temperature at −10 °C, the cell was started with the current step from 0 to 100 mA cm^{-2}, but the cell failed to start if the current step was increased to 200 mA cm^{-2}. In the case of lower air stoichiometry and feed gas temperature, the cell also failed to start up. This may have been due to the cell not heating rapidly enough with the starting procedure to prevent fatal freezing of the product water inside the cell.

3.3. Effects of freezing temperature on fuel cell components

The morphology of fuel cell components from fresh, normal operation and operation at sub-zero conditions are compared in Figs. 6–8. Figs. 6–8 illustrate the difference in MEA, gas diffusion layer and membrane, with the damage observed in fuel cell after operation failure or performance degradation. Images of fresh samples are provided for reference and to illustrate the overall magnitude of the damage.

Fig. 6c and d illustrate the massive damage observed at an MEA taken from a failed MEA after running at chamber temperature of −15 °C. Water freezing has delaminated the catalyst layer from both the membrane (Fig. 6c) and GDL (Fig. 6d). Fig. 7 shows that some damage to the backing layer fibers and binder occurred in the failed MEA. Fig. 7c shows damage to carbon paper after sub-freezing operation; it does appear that damage is occurring to the backing layer coating, Teflon, and the binder structure on the carbon paper surface. It is apparent from Fig. 7c that the GDL, which traps or holds bulk water during operation, was damaged when exposed to freezing temperatures. Some minor damage to the backing layer Teflon coating and binder occurred when the GDL was exposed to freezing temperatures. Fig. 8 shows the damage to the membrane. In the low

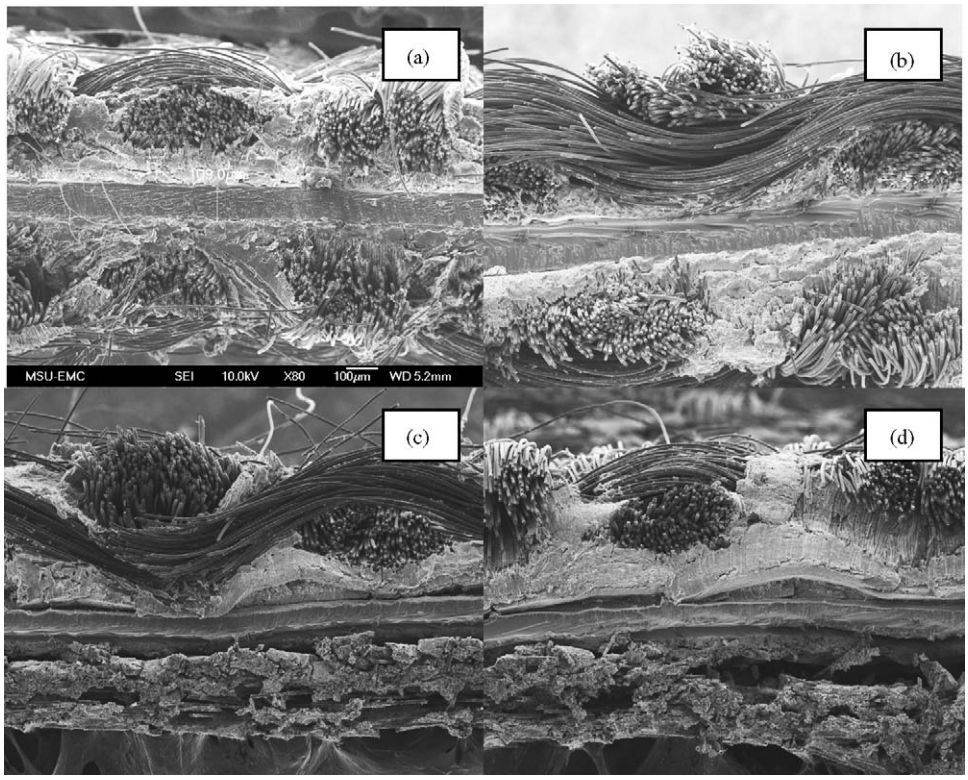

Fig. 6. Effect of sub-zero temperature on MEA. (a) Fresh MEA, (b) MEA after operation at room temperature, (c) MEA after operation at −10 °C and (d) MEA after operation at −15 °C.

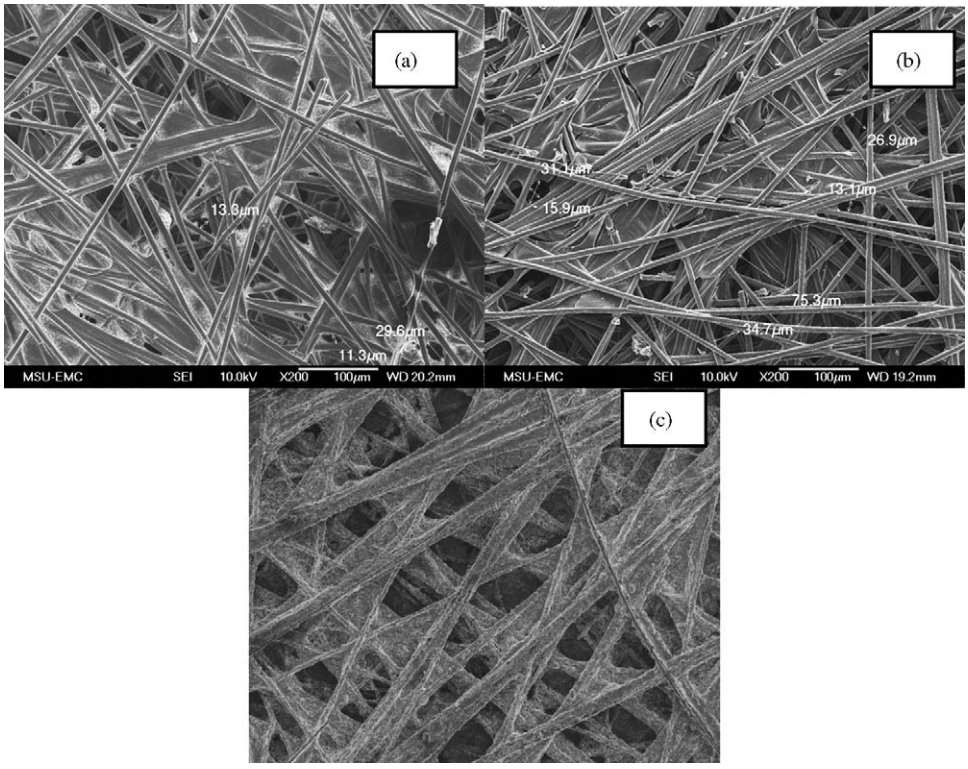

Fig. 7. Effect of sub-zero temperature on GDL. (a) Fresh carbon paper, (b) carbon paper after operation at room temperature and (c) carbon paper after operation at −15 °C.

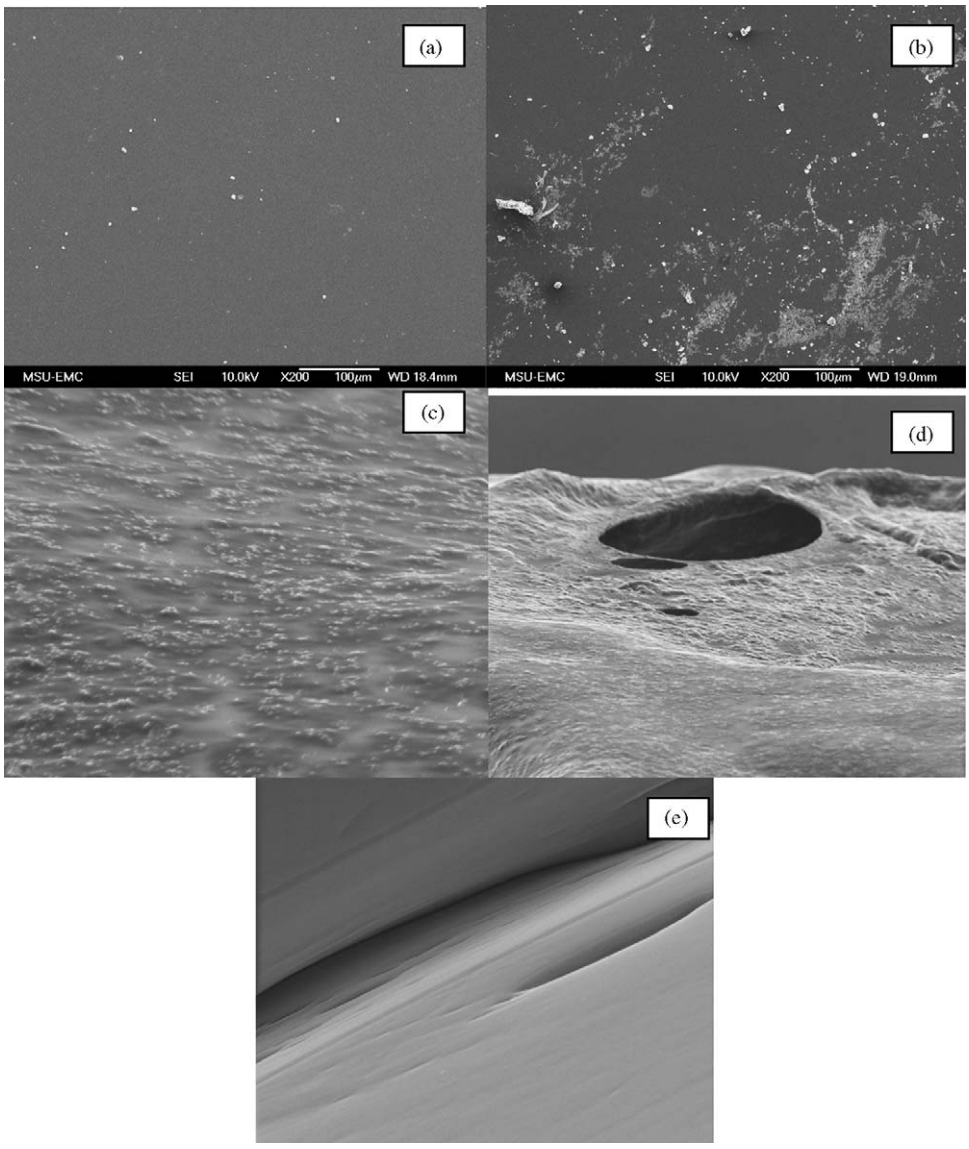

Fig. 8. Effect of sub-zero temperature on membrane. (a) Fresh Nafion membrane, (b) membrane after operation at room temperature, (c) membrane after operation at −15 °C, (d) membrane from cathode outlet regions after operation at −15 °C and (e) membrane from cathode outlet regions after operation at −15 °C.

magnification image, damage is present in the sample of the failed MEA as evidenced by the rough membrane surface after exposure to sub-zero freezing (Fig. 8c). In the high magnification image (Fig. 8d and e), the membrane does appear to show signs of pinhole damage (Fig. 8d) and micro-cracking (Fig. 8d) following operation at sub-zero temperatures.

4. Discussion

The properties of Nafion at freezing temperatures are important when considering the damage that may result to the membrane electrode assembly during operation at sub-zero temperatures due to the freezing of in situ water [21]. The state of water in Nafion has been classified into two categories [22–24], non-freezing and freezing bound, while there are three states for water present on membrane surface: non-freezing, freezing bound, and free water (bulk water). Free water does not have chemical interactions with the ions in the membrane and will freeze at around 0 °C. By means of differential scanning calorimetry and IR spectroscopy, Xie and Okada [25] demonstrated that there are two types of water in the Nafion membrane: one type that does not freeze, and one type that freezes. He found that freezing water molecules interacted weakly with the cations and ion exchange sites, and froze at ∼−20 °C, behaving similarly, but not identically to bulk water. He also found that non-freezing water molecules could not be solidified to ice even at −120 °C, and he considered these water molecules that were strongly bound with the cations and the ion exchange sites and exposed to the fluorocarbon environment. Okada et al. concluded that membrane damage could not be due to water inside the Nafion membrane, but may occur from the freezing of water on the membrane surface. A portion of the bulk water may exist in the interface between membrane and catalyst layer if fuel cell is running under sub-zero temperature conditions or if the fuel

cell is not purged before it is shut down. Therefore, ice formation may occur on the membrane surface, resulting in damage. This type of damage was identified in the membrane in this work through use of scanning electron microscopy (SEM), as shown in Fig. 8 and discussed in Section 3. The catalyst layer and gas diffusion layer (GDL) are both porous and permeable to gases while the membrane is non-porous and impermeable to gases. Water confined in porous materials can exist as free water (bulk water), bound water and bound–non-freezing water. Hayashi et al. [26] classified water absorbed in porous coal into three types, each exhibiting different properties; free water (freezes around 273 K), bound water (freezes between 213 and 260 K), and water that will not freeze. The temperature at which water freezes is affected by the pore size which contains the water and the properties of the porous material. Based on the Gibbs–Thompson equation [26], bound water and non-freezable water should be present in pores with diameters smaller than 10 nm. The authors also analyzed the freezing point temperature distribution of bound water in coal on the basis of the Gibbs–Thompson equation. The electric permittivity of water decreases significantly after water freezes [27], Sliwinska-Bartkowiak et al. [28] used dielectric relaxation spectroscopy to determine the melting point of water in active carbon fibers with a mean pore diameter around 1.8 nm. They found that the capacitance of the system changed significantly with the water phase transition at 273 K (0 °C) (bulk freezing temperature) and at 235 K (−38 °C) (corresponding to water crystal formation inside the pores).

Pore sizes in the catalyst layer and in the carbon paper/cloth used for the gas diffusion layer range from several nanometers (nm) to several hundred micrometers (μm). The pore size significantly affects the water freeze–thaw process in MEAs. These micro-porous media could hold significant amounts of water in the cathode side while the fuel cell is operating. A portion of water can freeze if the fuel cell is running at a temperature below zero, or if the fuel cell is not purged before it is shut down. This is due to water generation at the cathode by the oxygen reduction reaction (ORR). Thus, bulk water can exist in the porous catalyst layer and GDL at temperatures below zero. Freezing of the water in the porous micro-structure of the catalyst layer and/or GDL may result in damage due to the increased volume occupied by ice, compared to liquid water. Damage of this nature to the MEA was evident in the SEM results (Figs. 6–8). The SEM micrographs demonstrate that catalyst layer delamination from both membrane and gas diffusion layer occurred as a result of the sub-zero temperature. These interfacial delaminations play a major role in fuel cell performance loss under sub-freezing conditions. The SEM micrographs also show that the morphology of the porous carbon material was changed after exposure to sub-zero temperatures. For the system components examined as fresh or after exposure to normal operating conditions, the GDL surface was smooth. After exposure to sub-zero temperatures, the GDL surface was porous and dark in color. This may be due to ice formation in the GDL damaging the microstructure of the Teflon coating. This may result in changes in GDL gas permeability and electron conductivity as a result of exposure to sub-zero temperatures and will be detrimental to fuel cell performance.

5. Conclusions

The effect of sub-zero temperatures on the performance of a PEMFC was studied. Polarization curves were measured at chamber temperatures between 80 and −15 °C. The cell cathode temperatures were also recorded when each polarization curve was measured. Fuel cell performance at chamber temperatures of 25, 0, −5 and −10 °C was stable and reproducible. The cell temperature fluctuated as the current was scanned, with fluctuations between 2 and 3 °C. The cell temperature, however, achieved a stable shape. The fuel cell cathode temperature at chamber temperatures of 25, 0, −5 and −10 °C was stable and reproducible. However, at a chamber temperature of −15 °C, fuel cell performance was unstable. After four cycles, the cell voltage was decreased and suddenly collapsed to zero at a current density of 350 mA cm^{-2}. This sudden collapse occurred with the cathode temperature below −5 °C. The cathode temperature was unstable and suddenly dropped sharply to −15 °C.

Cell cold-start was investigated at temperatures of −5, −10 and −15 °C. Results demonstrated that a single cell was able to start at −5 °C if the cell was pre-purged and insulated. If the fuel cell was shut down without purge, it could not be subsequently started up. The cell was capable of starting operation with the proper starting procedure at −10 °C. With the higher air stoichiometry and higher feed gas temperature at −10 °C, it was possible to start up the cell using a current step from 0 to 100 mA cm^{-2}. However, if the current step was 0–200 mA cm^{-2}, the cell failed to start up. SEM results illustrated that the MEA, gas diffusion layer and membrane in the fuel cell were damaged leading to system failure or performance degradation. Delamination of the catalyst layer from both the membrane and GDL was found have occurred in the MEAs exposed to sub-zero temperatures during operation. Minor damage to the backing layer Teflon coating was also found.

Acknowledgement

This project was supported by the Center for Advanced Vehicular Systems (CAVS) at Mississippi State University.

References

[1] D. Oliver, J. Murphy, G. Duncan Hitchens, D.J. Manko, J. Power Sources 47 (1994) 353–368.
[2] S.J.C. Cleghorn, X. Ren, T.E. Springer, M.S. Wilson, C Zawodzinski, T.A. Zawodzinski, S. Gottesfeld, Int. J. Hydrogen Energy 22 (1997) 1137–1144.
[3] K.B. Prater, J. Power Sources 61 (1996) 105–109.
[4] S. Srinivasan, R. Mosdale, P. Stevens, C. Yang, Annu. Rev. Energy Environ. 24 (1999) 281–328.
[5] P. Seshadri, Z. Kabir, in: R.K. Shah, E.U. Ubong, S. Samuelsen (Eds.), Third International Conference on Fuel Cell Science, Engineering, and Technology, Proceedings, Ypsilanti, MI, United States, May 23–25, 2005, 2005, pp. 733–738.
[6] M. Gummalla, H. Gupta, S. Ghosh, S. Burlatsky, P. Hagans, C. Rice, AIChE Annual Meeting, Conference Proceedings, Austin, TX, November 7–12, 2004, 2004, pp. 023A/1–023A/7.
[7] M. Sundaresan, R.M. Moore, J. Power Sources 145 (2) (2005) 534–545.
[8] M. Oszcipok, D. Riemann, U. Kronenwett, M. Kreideweis, M. Zedda, J. Power Sources 145 (2) (2005) 407–415.

[9] E.A. Cho, J.J. Ko, H.Y. Ha, S.A. Hong, K.Y. Lee, T.W. Lim, I.H. Oh, J. Electrochem. Soc. 150 (2003) A1667.
[10] E.A. Cho, J.J. Ko, H.Y. Ha, S.A. Hong, K.Y. Lee, T.W. Lim, I.H. Oh, J. Electrochem. Soc. 151 (2004) A661.
[11] J. Cargnelli, P. Rivard, D. Frank, R.B. Gopal, Fuel cell for deployable applications in sub-zero environment, Portable Fuel Cells (1999).
[12] D. Chu, R. Jiang, K. Gardner, R. Jacobs, J. Schmidt, T. Quakenbush, J. Stephens, Polymer electrolyte membrane fuel cells for communication applications, J. Power Sources 96 (2001).
[13] B.K. Datta, G. Velayutham, A.P. Goud, Fuel cell power source for a cold region, J. Power Sources 106 (2002).
[14] F. Kagami, T. Ogawa, Y. Hishinuma, T. Chikahisa, Simulating the performance of a PEFC at a temperature below freezing, in: Fuel Cell Seminar, 2002, Abstracts.
[15] F. Kagami, Y. Hishinuma, T. Chikahisa, Performance and selfstarting of a PEFC at temperatures below freezing, Thermal Sci. Eng. 10 (3) (2002).
[16] F. Kagami, T. Ogawa, Y. Hishinuma, T. Ghikahisa, Fuel Cell Seminar, 2002, p. 239.
[17] E.L. Thompson, R.L. Fuss, United States Patent 6,887,598 (2005).
[18] R.J. Assarabowski, W.T. Unkert, L.A. Bach, A.P. Grasso, B.O. Olsommer, United States Patent 6,797,421 (2004).
[19] A. Christen, J.T. Mueller, United States Patent 6,743,538 (2004).
[20] J. St.-Pierre, J. Roberts, K. Colbow, S. Campbell, A. Nelson, J. New Mater. Electrochem. Syst. 8 (3) (2005) 163–176.
[21] A. Mauritz, R.B. Moore, State of understanding of Nafion, Chem. Rev. 104 (10) (2004) 4535–4586.
[22] H. Yoshida, Y. Miura, J. Membr. Sci. 68 (1992) 1.
[23] M. Pineri, F. Volino, M. Escoubes, J. Polym. Sci., Polym. Phys. Ed. 23 (1985) 2009.
[24] N. Boyle, V.J. McBrierty, A. Eisenberg, Macromolecules 16 (1983) 80.
[25] G. Xie, T. Okada, Denki Kagakuoyobi Kogyo Butsuri Kagaku 64 (6) (1996) 718–726.
[26] J. Hayashi, K. Norinaga, N. Kudo, T. Chiba, Energy Fuels 15 (2001) 903–909.
[27] B. Szurkowski, T. Hilczer, M. Sliwinska-Bartkowiak, Ber. Bunsen-Ges. Phys. Chem. 97 (5) (1993) 731.
[28] M. Sliwinska-Bartkowiak, G. Dudziak, R. Sikorski, R. Gras, K.E. Gubbins, R. Radhakrishnan, Phys. Chem. Chem. Phys. 3 (2001) 1179–1184.